Circumferential magnetization curves of Co-rich amorphous wires under tensile stress

M. T. González, K. L. García, and R. Valenzuela[a)]
Institute for Materials Research, National University of Mexico, P.O. Box 70-360, México D. F. 04510 Mexico

(Received 25 June 1998; accepted for publication 28 September 1998)

Circumferential magnetization curves were obtained for low, negative magnetostriction amorphous wires of nominal composition $(Co_{0.94}Fe_{0.06})_{72.5}B_{15}Si_{12.5}$, under tensile stress up to 250 MPa, by using the magnetoimpedance effect. The various magnetization processes, i.e., spin rotation, domain wall bulging, and domain wall displacement were resolved by frequency measurements in the 5 Hz–13 MHz range, and by varying the applied field amplitude between 0.28 and 12 A/m (root mean square). The results show that reversible magnetization processes (domain wall bulging and spin rotation) are damped by tensile stress, while the irreversible process (domain wall displacement) is enhanced by stress. These results are interpreted in terms of an increase in anisotropy and a reorienting of magnetization in circumferential domains, both as a result of the stress-induced anisotropy. © *1999 American Institute of Physics.* [S0021-8979(99)04501-6]

I. INTRODUCTION

Magnetoimpedance (MI) refers to the variations in the impedance response of amorphous ferromagnetic materials (submitted to a high-frequency current of small amplitude, i_{ac}) when a dc magnetic field, H_{dc}, is applied. This is a classic electromagnetic phenomenon[1] based essentially on the inductive coupling between the small ac field, H_{ac}, generated by the current flowing through the material and its magnetic structure. It is usually interpreted by considering that at high frequencies, the penetration depth of the ac field decreases by the skin-depth effect, and an additional contribution to the total impedance appears. As the dc field is applied, the effective permeability value decreases, the skin depth increases, and its contribution to the total impedance decreases. MI has generated considerable interest for applications in magnetic field sensor technology.[2–4]

The active magnetization processes depend on the particular domain structure of the sample, but also on the amplitude and frequency of the small ac field generated by the ac current. The inductive coupling is larger for materials with a transverse domain structure since the applied field is parallel to domain walls. Dc fields (originated by dc currents) have been observed to produce domain wall displacements;[5] for lower fields, domain wall bulging has also been observed.[6]

In the case of ac fields on Co-rich wires, a relaxation behavior of the complex permeability has been reported.[7] For field frequencies lower than the relaxation value, f_x, evidence of a threshold field, H_p, separating the low-field, reversible magnetization range (due to domain wall bulging) from the irreversible, hysteretic range (due to domain wall displacements) has been observed.[7] For frequencies above the relaxation value, domain walls are unable to follow the field, and spin rotation is then the only magnetization process available.[8]

When an external dc field is applied, domain wall movements are damped,[9] the inductive coupling is reduced, and its impedance contribution is strongly decreased. If H_{dc} is high enough to saturate the sample, its total impedance decreases to a value close to that of a nonferromagnetic material. In the absence of domain walls, only spin rotation remains as the magnetization process; ferromagnetic resonance has been effectively observed[10] at high frequencies in amorphous wires.

The magnetoelastic behavior of MI is currently being investigated[11–13] for potential applications in gauge sensors, as well as for its own scientific interest. However, these studies seem inconclusive; in particular, the key role played by the ac current amplitude is neglected, and results do not appear directly correlated with the corresponding magnetic structures. A combination of the skin-depth effect and tensile stress has not been clearly established. Also, in most literature on MI, the results are given in the impedance (total or complex) formalism, which does not show clearly the magnetic nature of the phenomenon.

In this article, we present a study of the effects of tensile stress on the impedance response of CoFeBSi amorphous wires in the as-cast state. The inductance formalism, which provides a direct image[14] of magnetic phenomena, it used. By analyzing the complex inductance response as a function of the ac circumferential field (produced by the ac current flowing through the wire) at selected frequencies, circumferential magnetization curves are derived. It is found that reversible magnetization processes (i.e., domain wall bulging and spin rotation) are damped by stress, while irreversible, hysteretical processes (domain wall displacements) are enhanced by stress. An interpretation of these results in terms of the stress-induced anisotropy is proposed.

II. EXPERIMENTAL TECHNIQUES

We used pieces of 10 cm long amorphous wires of nominal composition $(Co_{0.94}Fe_{0.06})_{72.5}B_{15}Si_{12.5}$ in the as-cast state, kindly provided by Unitika Ltd., Japan. These wires were placed in a weight and pulley system to apply tensile stresses

a)Corresponding author; electronic mail: monjaras@servidor.unam.mx

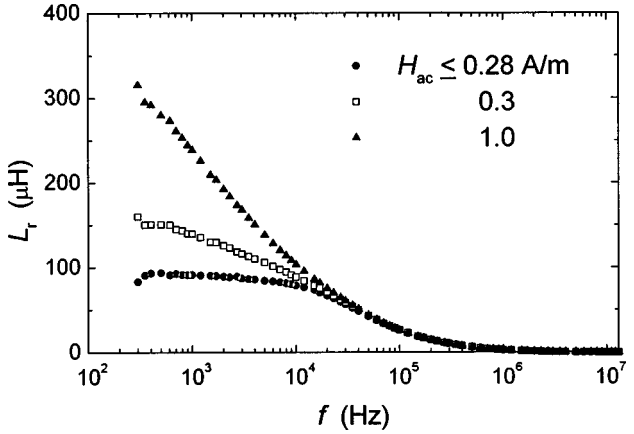

FIG. 1. Real part of inductance, L_r, as a function of frequency for selected field amplitudes and $\sigma=0$.

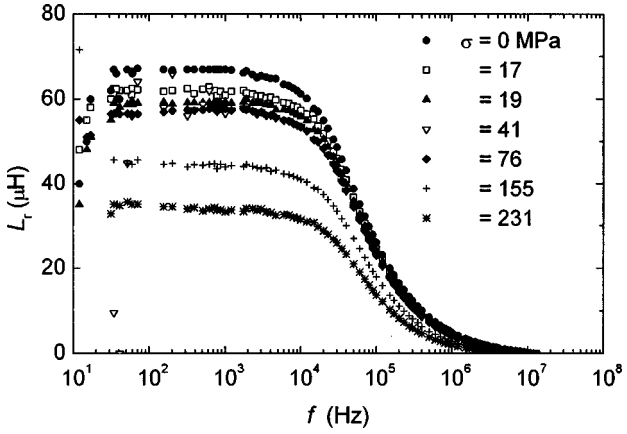

FIG. 2. Real part of inductance, L_r, as a function of frequency for several values of tensile stress.

up to 250 MPa. This system allows a good electrical contact on the wire ends (previously cleaned with a soft acid solution) to apply the ac current.

Impedance measurements were carried out at room temperature with a system including a HP 4192 A impedance analyzer in the 5 Hz–13 MHz frequency range. The amplitude of the ac current was varied between 0.22 and 9.6 mA [root mean square (rms)]; the ac field generated by these currents in a radial point R of the wire is given by

$$H_{ac}=i_{ac}R/(2\pi A^2), \tag{1}$$

where A is the wire's radius, and leads to circumferential fields between 0.28 and 12 A/m (rms) on the wire surface, where it is maximum.

III. RESULTS

The use of the complex inductance formalism, $L=L_r+jL_i$, instead of the complex impedance formalism, $Z=Z_r+jZ_i$, [where $j=(-1)^{1/2}$ and the r and i subindices indicate the real and imaginary components, respectively], leads to a clearer physical picture of the magnetization processes involved in ferromagnetic materials. Complex inductances are obtained from impedances by

$$L=(-j/\omega)Z, \tag{2}$$

where ω is the angular frequency ($\omega=2\pi f$) and $j=(-1)^2$. Note that the presence of j in this transformation leads to an exchange of real and imaginary parts: the real inductance depends on the imaginary impedance, and conversely, the imaginary part of inductance is given by the real impedance. Complex permeability is derived from complex inductance by means of the pertinent geometrical constant, G, as $\mu=GL$. For a wire of length, l, G is given (in SI units, henry^{-1}) as, $G=10^7/l$.

We first determined the domain wall propagation field, H_p, which separates the reversible magnetization range (initial permeability) from the irreversible, hysteretic range, by measuring frequency scannings at increasing field amplitudes. The value of H_p can be obtained from L_r vs f plots, as shown in Fig. 1.

For ac fields lower than, or equal to, the propagation field, the real part of inductance, L_r, exhibits a low-frequency plateau, followed by a relaxation dispersion, f_x. The value f_x of our samples is about 40 kHz. At $f<f_x$, the real part of inductance is reversible and independent of frequency and field amplitude, which is in agreement with the bulging behavior of pinned domain walls normally attributed to initial permeability.

For $H_{ac}>H_p$ the low-frequency value of L_r is no longer a constant, but becomes field and frequency dependent (Fig. 1), increasing at low frequencies with field amplitude, but decreasing as a function of frequency. This behavior can be ascribed to the irreversible character of hysteresis for $H_{ac}>H_p$, corresponding to domain wall unpinning and displacement. The observed value for the propagation field is $H_p=0.28$ A/m (rms). As frequency increases, all the curves merge into a single one showing the domain wall relaxation.

We then carried out experiments as a function of the tensile stress, σ, for the reversible magnetization range ($H_{ac}<H_p$). The tensile stress, σ, decreases the L_r values in the low-frequency range (see Fig. 2) where σ appears as a parameter.

Since the inductance values for the irreversible magnetization range ($H_{ac}>H_p$) depend on the field and frequency, we chose to investigate this field range at constant, selected frequencies of 1 kHz and 5 MHz, i.e., below and above, respectively, the relaxation frequency. As we have previously shown,[15] circumferential magnetization curves can be derived from L_r by transforming it to permeability, μ, and then to induction B, and finally to circumferential magnetization, M, by using the pertinent general relations [$\mu=B/H$; $B=(H+M)\mu_0$; $\mu_0=$permeability of vacuum]. Circumferential magnetization curves for several stress values were then obtained for both frequencies.

For the 1 kHz experiments, circumferential magnetization curves showed an increase as a result of σ, as shown in Fig. 3. The tensile stress therefore favors the magnetization process at these frequencies.

At 5 MHz, circumferential magnetization curves exhibited a virtually linear behavior, with a slope decreasing as the applied stress increased (Fig. 4). In contrast with the magne-

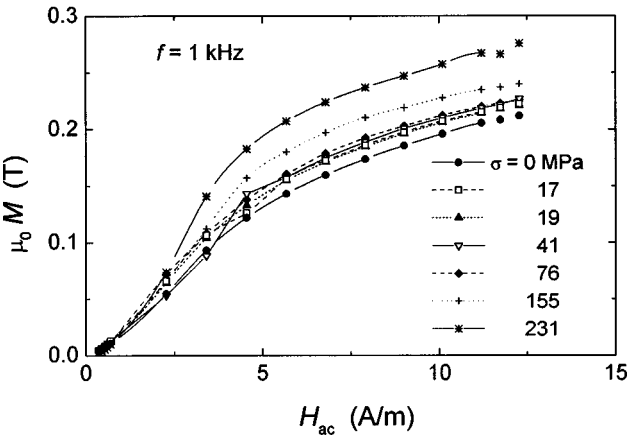

FIG. 3. Circumferential magnetization curves at $f=1$ kHz for several tensile stress values. Both the magnetization and the applied field values are rms values (the curves are drawn to guide the eye only, and do not represent any model).

tization behavior at 1 kHz, tensile stress opposes the magnetization process at 5 MHz.

The experiments at $H_{ac}<H_p$ and those at $f=5$ MHz have one thing in common: they are associated with reversible magnetization mechanisms. The former depends mainly on the bulging of pinned domain walls, and the latter is associated with spin rotation, since this frequency is clearly larger than the domain wall relaxation frequency. Reversible magnetization processes are therefore damped by stress. In the case of irreversible magnetization mechanisms (experiments at $H_{ac}>H_p$ and at $f=1$ kHz), results show the opposite: magnetization values increases as the sample is submitted to increasing tensile stress.

IV. DISCUSSION

We consider first the experiments carried out at 5 MHz. This frequency is well above the relaxation frequency ($f_x \approx 40$ kHz) of domain walls, and magnetization can take

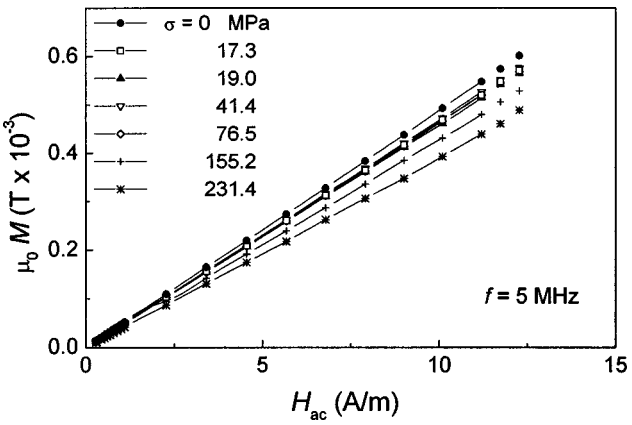

FIG. 4. Circumferential magnetization curves at $f=5$ MHz for several tensile stress values. Both the magnetization and the applied field values are rms values (the curves are drawn to guide the eye only, and do not represent any model).

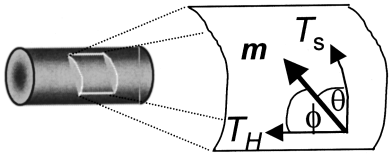

FIG. 5. Geometry of magnetization, M_s, and torques, T_s and T_h, produced by the tensile stress and the ac applied field, respectively, in the outer shell of the wire.

place only by the spin rotation process. In order to evaluate the possible effects of a limited field depth penetration, δ, we utilize the usual relationship

$$\delta=(\rho/\pi\mu f)^{1/2}, \tag{3}$$

where ρ is the resistivity, μ is the magnetic permeability, and f is the frequency of the applied field. For this calculation, we used values of rotational permeability obtained from experiments in the magnetically saturated state of the wire. The wire was submitted to axial dc fields of 6.4 kA/m (80 Oe) and a run over the frequency range was carried out. The real part of inductance showed a constant value above 8 μH, insensitive to both the amplitude and frequency of the ac field. The relative rotational permeability can then be calculated as $\mu_{rel}=GL=800$; the absolute value is therefore $\mu_{rot}=1.01\times10^{-3}$ H/m. The value of the resistivity can be derived from our values of real impedance at low frequency, leading to $\rho=1.90\times10^{-4}$ Ω m. Finally, with $f=5$ MHz, a value of $\delta=109$ μm is obtained by using Eq. (3). Since the wire's diameter is 62 μm, no correction for skin-depth effects is needed.

The effects of stress on magnetic susceptibility were first analyzed by Becker and Kersten[16] by considering the magnetoelastic energy, E_σ,

$$E_\sigma=(3/2)\lambda_s\sigma(\sin\theta)^2, \tag{4}$$

where λ_s is the saturation magnetostriction constant and θ is the angle between the magnetization direction and the stress axis. On the other hand, the magnetic potential energy, E_H, due to the applied field, H, is given by

$$E_H=-\mu_0 H M_s\cos\phi, \tag{5}$$

where μ_0 is the permeability of vacuum and ϕ is the angle between the magnetization axis and the applied field direction. The investigation of the magnetic domain structure of Co-rich wires has led to a simple[17] model: an inner core with axially oriented domains, and an outer shell formed by domains with circumferential magnetization (with an alternate orientation in the nonmagnetized state). With this model in mind, we consider the geometry shown in Fig. 5, where the magnetization vector, M_s, of a circumferential domain in the outer shell is submitted to both the circumferential ac field, H_{ac}, produced by the ac current, and the stress σ. Since this composition in the as-cast state possesses a negative saturation magnetostriction constant[18] ($\lambda_s=-0.4\times10^{-7}$), the tensile stress exerts a torque on M_s,

$$T_\sigma=\partial E_\sigma/\partial\theta=(3/2)\lambda_s\sigma 2\cos\theta\sin\theta, \tag{6}$$

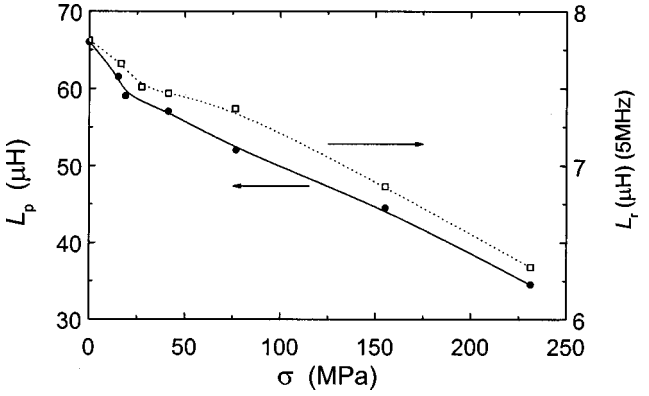

FIG. 6. Effect of tensile stress on the real part of inductance, L_r, measured at 5 MHz, and on the equivalent inductor value, L_p.

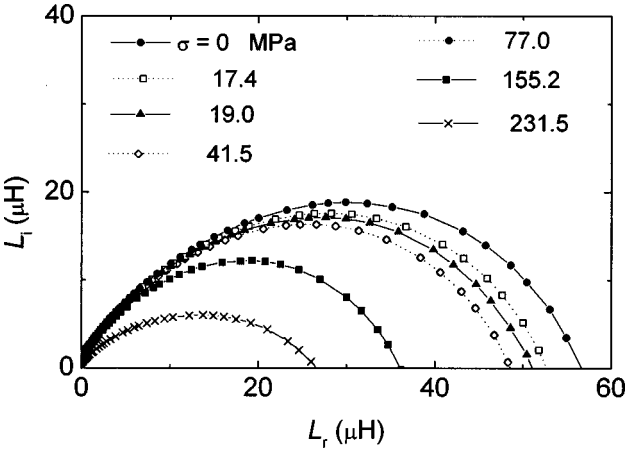

FIG. 7. Complex plot of inductances for $H_{ac}<H_p$ as a function of tensile stress.

which tends to maintain it perpendicular to the stress axis, i.e., in the circumferential orientation.

The effect of the ac field can also be considered as a torque, T_H; during the first half period, this torque also maintains M_s in the (up) circumferential position. For the second half period, however, the ac field is reversed, and the torque is exerted in the opposite (down) circumferential direction. For this simplified approximation, we assume that M_s rotates in the cylindrical surface of Fig. 5, and consider that the most significant magnetization process is the rotation of M_s from the initial (up) circumferential direction to the axial position only since, once this condition has been reached, the magnetization vector simply completes the rotation to the down position without any need to increase the ac field. The magnetic field torque can then be written as

$$T_H = \partial E_\sigma / \partial \phi = \mu_0 M_s H_{ac} \sin \phi. \tag{7}$$

The equilibrium position of the magnetization vector is $T_H = T_\sigma$, which together with the geometrical condition $\theta + \phi = 90°$ leads to

$$3\lambda_s \sigma \sin \phi \cos \phi = \mu_0 H_{ac} M_s \sin \phi, \tag{8}$$

and therefore,

$$H_{ac} = 3\lambda_s \sigma \cos \phi / \mu_0 M_s. \tag{9}$$

Since the magnetization component in the field torque direction is $M = M_s \cos \phi$, and the susceptibility, χ, is defined as M/H,

$$\chi = \mu_0 M_s^2 / 3\lambda_s \sigma, \tag{10}$$

it appears that the rotational susceptibility (and permeability for a highly permeability material) is inversely proportional to stress. Our results of real inductance, L_r, as a function f stress (which were used to obtain the magnetization curves at $f = 5$ MHz in Fig. 4) appear in Fig. 6. A decrease of L_r with σ is observed, although the functional form is closer to a linear relation, instead of the hyperbolic form of Eq. (10).

We move now to the low-frequency ($f = 1$ kHz) measurements. A calculation of the field penetration depth should be carried out in order to assess if this correction is needed. Equation (3) is used now with $f = 1$ kHz and a value of permeability calculated from the highest L_r values at the lowest frequency (see Fig. 1), $L_r = 300$ μH. The calculated (absolute) permeability under these conditions is about 0.0377 H/m, which leads to $\delta = 1267$ μm, clearly larger than the wire's diameter.

The low-frequency, low ac field amplitude (for $H_{ac} < H_p$) results are now considered. It has been shown[7,14,19] that the inductance behavior of a wide variety of ferromagnetic materials can be modeled to a good approximation as a simple equivalent circuit: a series $R_s L_s$ circuit in series with a parallel $R_p L_p$ arrangement. The series inductor is associated with the rotational permeability and the series resistor is the wire's dc resistance. The parallel section represents the reversible bulging of domain walls, with the parallel inductor associated with the initial permeability and the parallel resistor associated with the domain wall viscous damping coefficient.

It can be shown that for the parallel circuit the locus of the L_r and L_i values on the complex plane for a wide ensemble of f values is a semicircle, as shown in Fig. 7. Also, a spectroscopic plot of the real and imaginary parts of inductance showed a relaxation dispersion and a maximum at the relaxation frequency, respectively, as shown in Fig. 8.

The value of circuit elements can be extracted from data as follows: L_p is the semicircle's diameter; f_x corresponds to

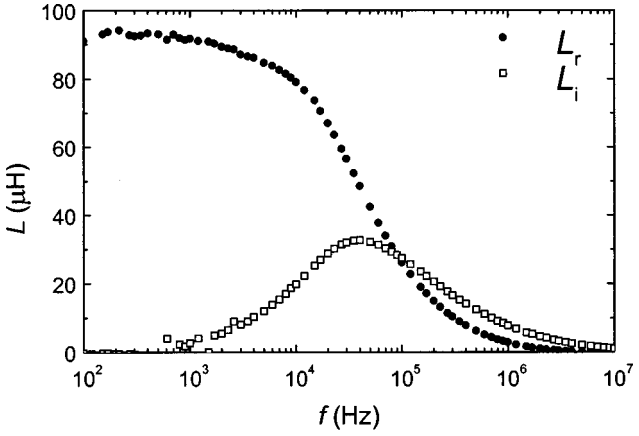

FIG. 8. Behavior of the real and the imaginary parts of inductance as a function of frequency at zero stress.

the condition $L_r = L_i$, and can be extracted from the maximum in L_i-f plots; and, finally, the equivalent resistor is calculated from $R_p = \omega_x L_p = 2\pi f_x L_p$. The values of the equivalent circuit elements L_p, f_x, and R_p, as a function of the applied stress σ are presented in Figs. 6, 9, and 10, respectively.

The equivalent inductor L_p is associated with the circumferential initial permeability of the wire. Since it is extracted from the semicircle's diameter for each stress value, it is independent of frequency; this is consistent with the notion of an ideal element. Therefore, it is not affected by the field penetration depth phenomenon. L_p showed a decrease as a result of tensile stress (Fig. 6), whereas relaxation frequency exhibited an increase. It has been found (in amorphous ribbons submitted to longitudinal fields) that, when the free-bulging area of domain walls change, the variations in f_x and L_p compensate each other and R_p results in a constant value.[20,21] In the present case, L_p shows a decrease (Fig. 6) and f_x exhibits an increase (Fig. 9). Both results would point to a decrease in the free-bulging area of domain walls. However, R_p is not a constant but, rather, exhibits a decrease as a function of the applied stress (Fig. 10). This can be interpreted as a change in the intrinsic properties of walls, and not only as variations in the bulging area of domain walls. Since these amorphous wires possess a negative saturation magnetostriction constant, the observed results are consistent with an increase in induced anisotropy. Such an increase in anisotropy produces an increase in the damping factor of circumferential domain walls, and therefore, a decrease in their initial permeability. To a large extent, domain wall bulging is also a kind of (collective) spin rotation, and the effects of tensile stress can therefore be ascribed to a behavior similar to the one described by Eq. (10) shown in Fig. 6, where both rotational and bulging inductances are plotted as a function of stress.

The deviations of the experimental results from a perfect semicircle in complex plots (Fig. 7) have been studied in the case of electrical polarization phenomena.[22] The basic assumption is that the impedance response of a material is produced by a collection (or an ensemble) of impedance sources, and it is necessary to consider a distribution of time

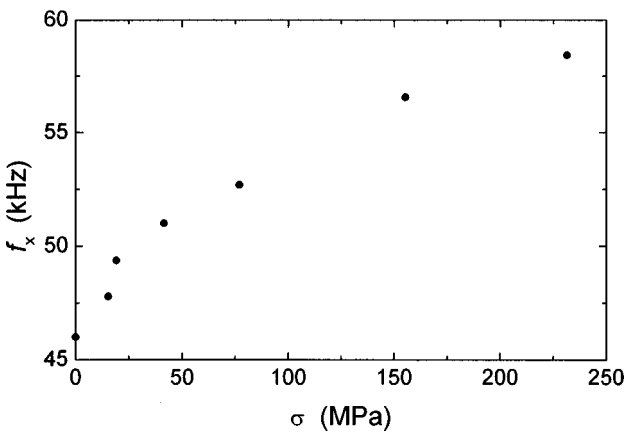

FIG. 9. Behavior of the relaxation frequency, f_x, as a function of stress.

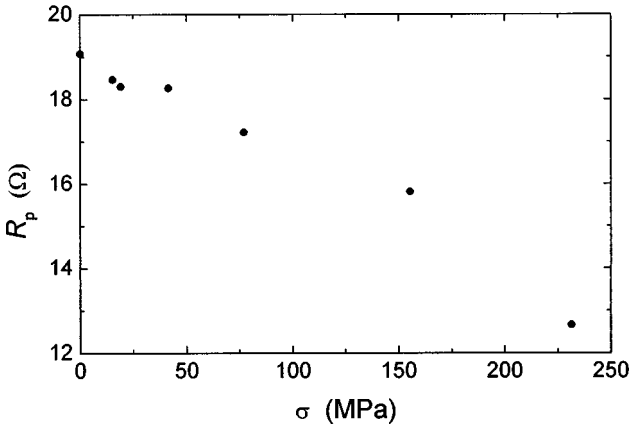

FIG. 10. Effect of stress on the equivalent resistor values, R_p.

constants, instead of a single time constant, τ. To our knowledge, distributed time constants in magnetic permeability have not been discussed. We assume that our experimental results (at $H_{ac} < H_p$ and $f = 1$ kHz) can be approximated by a $R_p L_p$ parallel circuit, recall the definition of the time constant, $\tau = L_p/R_p = 1/\omega_x$. A distribution in time constants can arise from variations in L_p, which in turn, result from a distribution in the pinning of circumferential domain walls.

Experiments at 1 kHz and $H_{ac} > H_p$ are associated with circumferential domain wall displacements as the dominant magnetization process. The observed increase in magnetization when the tensile stress is applied (Fig. 3) can be interpreted in ferromagnetic materials with negative magnetostriction as a consequence of the fact that mechanical stress assists the irreversible magnetization processes by favoring the reorientation of domains with magnetization in a direction different to that of the applied field.

In the simple inner-core and outer-shell domain structure model[17] for these wires, outer-shell domains are assumed to have a circumferential orientation. Our results show therefore that this domain orientation is not perfectly circumferential (which was recently suggested[23]). The tensile stress results in a better circumferential alignment of spins and leads therefore to higher magnetization values.

V. CONCLUSIONS

(a) Magnetization processes in circumferential domains of low magnetostriction, amorphous Co–Fe wires have been resolved, and the effects of tensile stress have been investigated separately on each of them.

(b) Tensile stress increases the damping of the reversible processes of domain wall bulging and spin rotation, while it enhances the irreversible displacement of domain walls.

(c) These results are interpreted in terms of a stress-induced anisotropy, leading to a decrease in reversible magnetization processes; for the irreversible process, a reorientation of nonideally oriented circumferential domains results in an increase of magnetization.

(d) Skin-depth penetration phenomena were not significant at the conditions investigated.

ACKNOWLEDGMENTS

The authors thank Dr. M. L. Sánchez (Oviedo, Spain) for helpful discussions on the magnetic calculations. This work was partially funded by CONACyT, Mexico, under Grant No. 3101P-A9607. One of the authors (M.T.G.) thanks DGAPA-UNAM, Mexico, for a fellowship under Grant No. IN100996.

[1] R. S. Beach and A. E. Berkowitz, Appl. Phys. Lett. **64**, 3652 (1994).
[2] P. T. Squire, D. Atkinson, M. R. J. Gibbs, and S. Atalay, J. Magn. Magn. Mater. **132**, 10 (1994).
[3] K. Mohri, T. Uchiyama, and L. V. Panina, Sens. Actuators A **59**, 1 (1997).
[4] M. Vázquez, M. Knobel, M. L. Sánchez, R. Valenzuela, and A. P. Zhukov, Sens. Actuators A **59**, 20 (1997).
[5] J. D. Livingston and W. G. Morris, J. Appl. Phys. **57**, 3555 (1985).
[6] J. D. Livingston, W. G. Morris, and T. Jagielinski, J. Appl. Phys. **55**, 1790 (1984).
[7] K. L. García and R. Valenzuela, Mater. Lett. **34**, 10 (1998).
[8] H. J. de Wit and M. Brouha, J. Appl. Phys. **57**, 3560 (1985).
[9] K. L. García and R. Valenzuela, IEEE Trans. Magn. **34**, 1162 (1998).
[10] A. Yelon, D. Ménard, M. Britel, and P. Ciureanu, Appl. Phys. Lett. **69**, 3084 (1996).
[11] M. Knobel, M. L. Sánchez, J. Velázquez, and M. Vázquez, J. Phys.: Condens. Matter **7**, L115 (1995).
[12] D. Atkinson and P. Squire, IEEE Trans. Magn. **33**, 3364 (1997).
[13] M. Knobel, M. Vázquez, M. L. Sánchez, and A. Hernando, J. Magn. Magn. Mater. **169**, 10 (1994).
[14] R. Valenzuela, M. Knobel, M. Vázquez, and A. Hernando, J. Phys. D **28**, 2404 (1995).
[15] M. L. Sánchez, R. Valenzuela, M. Vázquez, and A. Hernando, J. Mater. Res. **11**, 2486 (1996).
[16] R. Becker and M. Kersten, Z. Phys. **75**, 660 (1930).
[17] Y. Yamasaki, K. Mohri, H. Kawamura, H. Takamura, and F. B. Humphrey, IEEE Transl. J. Magn. Jpn. **4**, 360 (1989).
[18] C. Gómez-Polo and M. Vázquez, J. Magn. Magn. Mater. **118**, 86 (1993).
[19] G. Aguilar-Sahagún, P. Quintana, E. Amano, J. T. S. Irvine, and R. Valenzuela, J. Appl. Phys. **76**, 7000 (1994).
[20] R. Valenzuela and J. T. S. Irvine, J. Appl. Phys. **72**, 1486 (1992).
[21] I. Betancourt and R. Valenzuela, IEEE Trans. Magn. **33**, 3973 (1997).
[22] J. R. MacDonald, *Impedance Spectroscopy* (Wiley, New York, 1987), pp. 34–42.
[23] H. Theuss, B. Hofmann, C. Gómez-Polo, M. Vázquez, and H. Kronmuller, J. Magn. Magn. Mater. **145**, 165 (1993).